Precise age of C33N-C32R magnetic-polarity reversal, San Juan Basin, New Mexico and Colorado

James E. Fassett and Maureen B. Steiner
1997, pp. 239-247. https://doi.org/10.56577/FFC-48.239

in:

Mesozoic Geology and Paleontology of the Four Corners Area, Anderson, O.; Kues, B.; Lucas, S.; [eds.], New Mexico Geological Society 48th Annual Fall Field Conference Guidebook, 288 p. https://doi.org/10.56577/FFC-48

This page is intentionally left blank to maintain order of facing pages.

PRECISE AGE OF C33N-C32R MAGNETIC-POLARITY REVERSAL, SAN JUAN BASIN, NEW MEXICO AND COLORADO

JAMES E. FASSETT[1] and MAUREEN B. STEINER[2]

[1]U.S. Geological Survey, P.O. Box 25046, MS 939, DFC, Denver, CO 80225; [2] Dept. of Geology and Geophysics, University of Wyoming, Laramie WY 82071

Abstract—Polarity-chron boundary C33n-C32r has been identified in the Upper Cretaceous continental Farmington Sandstone Member of the Kirtland Shale in Hunter Wash in the southwest part of the San Juan Basin of New Mexico, and in the marine Lewis Shale at Chimney Rock, Colorado, in the northeast part of the basin. Single- and multiple-crystal laser fusion $^{40}Ar/^{39}Ar$ ages of sanidine crystals from volcanic ash beds bracketing the C33n-C32r polarity reversal at Hunter Wash establish its age as 73.50 ± 0.18 Ma. The reversal apparently occurs within the *Baculites compressus* Western Interior ammonite zone and within the Edmontonian land-vertebrate faunal zone. An 8 Ma hiatus separates Cretaceous and Tertiary rocks in the southern San Juan Basin. These findings provide a precise new interpolated Late Cretaceous tie point for geologic time scales, provide the basis for the direct correlation of Western Interior ammonite zones to European open-ocean faunal zones, and establish the first direct tie between continental and marine fossil zones within the Western Interior of North America.

INTRODUCTION

The purpose of this study was to identify and determine the age of a Late Cretaceous (Campanian) polarity reversal in continental and marine strata and to clarify the age relations and stratigraphy of rocks adjacent to the Cretaceous-Tertiary boundary in the San Juan Basin of New Mexico and Colorado. Two principal sites of our study were Hunter Wash in the southwest part of the basin in New Mexico and Chimney Rock in the northeast part of the basin in Colorado (Fig. 1). These sites were selected because they contain well-exposed, continuous sections of the stratigraphic sequences in which the reversal occurs; they contain numerous datable volcanic-ash beds; they contain distinct faunas and (or) floras; and sample-collection levels at these sections can be precisely tied to an underlying basin-wide subsurface marker bed, the Huerfanito Bentonite Bed of the Lewis Shale (Fassett and Hinds, 1971). Moreover, because of the time-transgressive nature of deposition of these strata, the polarity reversal could be identified in coeval continental and marine rocks.

The continental section (Fig. 1) begins in the Hunter Wash drainage at 36°18.59'N lat., 108°11.01'W long., and ends at the head of a north-trending tributary of Hunter Wash at 36°21.87'N lat., 108°8.34'W long. (Alamo Mesa West 7.5' Quadrangle, New Mexico). The section traversed the upper part of the continental Upper Cretaceous Fruitland Formation, the Kirtland Shale, and the lower part of the Tertiary Ojo Alamo Sandstone. The strata dip at 0.7° to the northeast; the land surface dips gently to the southwest.

The Chimney Rock paleomagnetic section consists of four adjacent segments within the Chimney Rock 7.5' Quadrangle, Colorado. The principal segment is on the steep, southeast side of the narrow, Pictured Cliffs Sandstone-capped mesa containing the prominent monolith "Chimney Rock" at its northeasternmost tip. The traverse started at 37°11.2' N lat., 107°18.02' W long. in the offshore-marine Lewis Shale and ended at 37°11.48' N lat., 107°18.33' W long. in the middle-shoreface facies of the Pictured Cliffs Sandstone. The upper part of the section was sampled in three shorter segments: (1) middle and upper parts of the Pictured Cliffs

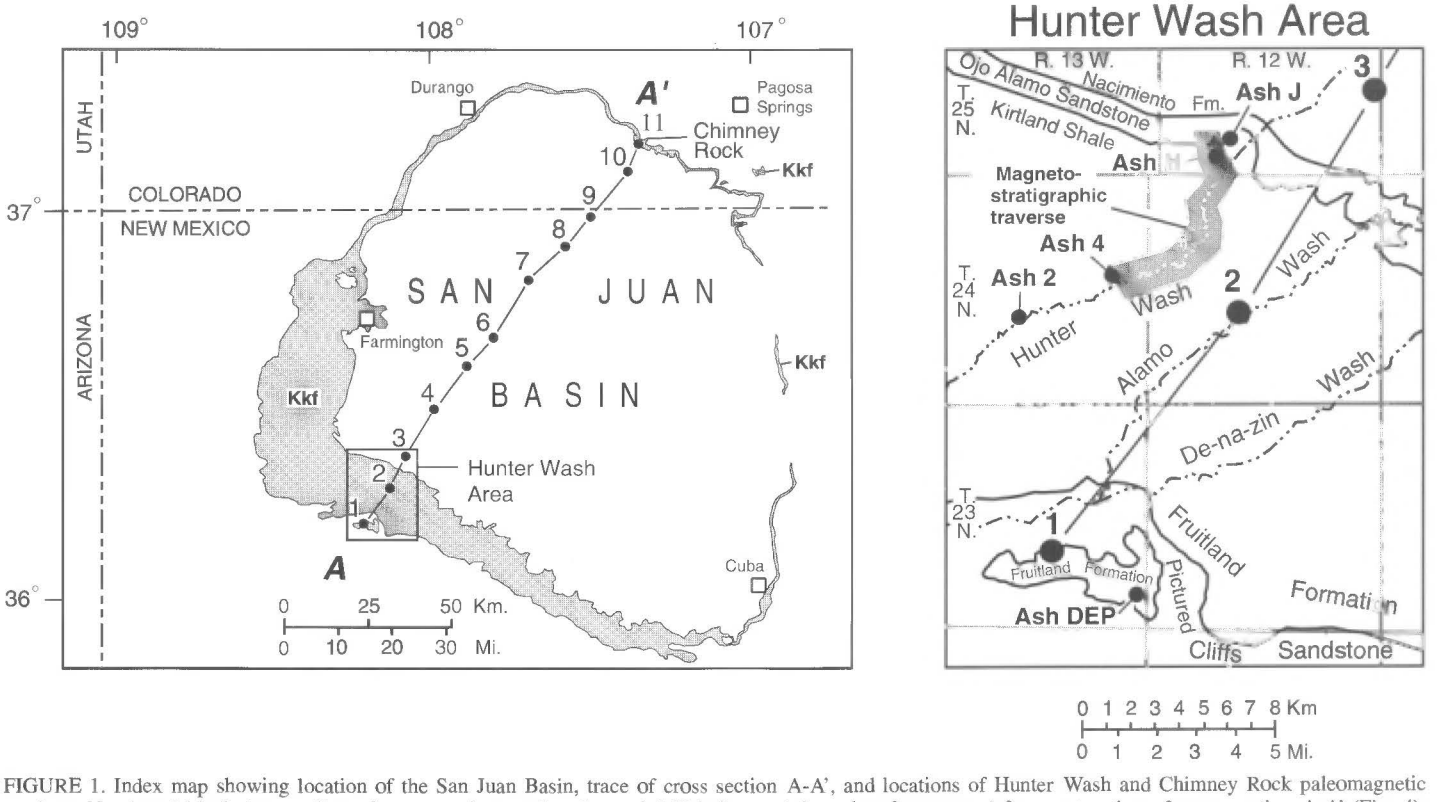

FIGURE 1. Index map showing location of the San Juan Basin, trace of cross section A-A', and locations of Hunter Wash and Chimney Rock paleomagnetic sections. Numbered black dots on line of cross section are locations of drill holes used for subsurface control for construction of cross section A-A' (Fig. 4); drill holes are listed in Table 2. Kkf is outcrop of Fruitland Formation and Kirtland Shale; ash-bed collection sites DEP, 2, 4, H, and J are shown on the large-scale map of the Hunter Wash area.

Sandstone in a cliff face on the south side of Colorado Highway 151 at 37°9.77' N lat., 107°19.02' W long.; (2) lowermost coal-bearing part of the Fruitland Formation on the west side of a small gully, near a small abandoned coal mine at 37°9.62' N lat., 107°18.38' W long.; and (3) lower Fruitland just above the main coal-bearing part in a low escarpment just south of Colorado Highway 151 at 37°9.62' N lat., 107°19.02' W long.

METHODS OF INVESTIGATION

Huerfanito Bentonite Bed datum

The Huerfanito Bentonite Bed is an altered volcanic ash bed in the Lewis Shale deposited in the Western Interior Seaway during late Campanian time, and thus is an isochronous datum. It forms a subsurface marker that is uniquely identifiable on geophysical logs throughout the San Juan Basin (Fassett and Hinds, 1971). In this report, paleomagnetic samples, dated ash beds, and paleontological collection sites are referred to in meters above the Huerfanito Bed in order to precisely compare and relate stratigraphic data obtained from different localities within the basin.

Paleomagnetism

Paleomagnetic samples at most sites were collected at 1–5 m intervals, although lithology and exposure dictated actual spacing. All samples were cored and oriented in the field. Generally, three or more samples per site were collected and measured. Thermal demagnetization was employed to separate characteristic and secondary magnetizations. A group of samples representative of all lithologies (shale, claystone, siltstone, and fine-grained sandstone) was treated in ten heating increments from 150°C to 375°C; thirty-five samples per stratigraphic section were treated in this detail. These data determined the treatment of the remainder of the samples, which then were thermally demagnetized in five steps: Hunter Wash samples at temperatures of 170°, 210°, 255°, 300° and 335°C, and Chimney Rock samples at 190°, 225°, 260°, 300° and 335°C. The magnetic behavior of Hunter Wash samples was nearly the same as that described by earlier studies from an adjacent location in Alamo Wash (Fig. 1) located 3 km east of Hunter Wash (Butler et al., 1977; Lindsay et al., 1981).

Only those samples yielding coherent demagnetization responses, consisting of a linear array of points, were included in the interpretations. Characteristic directions were determined by principal component analysis, utilizing three or more points per sample. Samples only responding to demagnetization with directions similar to that of the current geomagnetic field (14%) were excluded from the analysis. These samples may represent outliers of a population of Cretaceous directions or they may actually represent remagnetization in the present magnetic field; their exclusion results in some of the apparent gaps in sampling in Figures 2 and 3.

Hunter Wash

The initial directions of magnetization (mean = 358°, 54°, $alpha_{95}$ = 6°) largely clustered around the axial dipole field direction (0°, 55°; present field = 12°, 63°). Intensities of magnetization averaged 5 x 10^{-2} A/m. The magnetization lost in the first heating step (about 170° C) had directions near the axial dipole direction. The characteristic magnetization directions were generally revealed by thermal demagnetization between 200° and 300°C. Samples lost most of their magnetization by 350–375°C.

Much of the lower portion of the section displays normal polarity (Fig. 2). Above the sequence of samples of solidly normal polarity is an interval in which sample magnetizations appear to indicate three or more reversals of polarity in rapid succession. The overlying stratigraphic section exhibits clearly reversed polarity magnetization, which continues to the base of the Ojo Alamo Sandstone. The basal part of the Ojo Alamo also exhibits reversed polarity, whereas the upper portion mostly exhibits normal polarity.

Several aspects of Hunter Wash paleomagnetism indicate that the characteristic direction is that of the Cretaceous geomagnetic field. First, individual samples within a site generally exhibit remarkably similar magnetization behavior and characteristic directions. Second, the mean of the normal polarity sample directions (336.4°, 47.6°, $alpha_{95}$ = 4.6°, N=58) re-

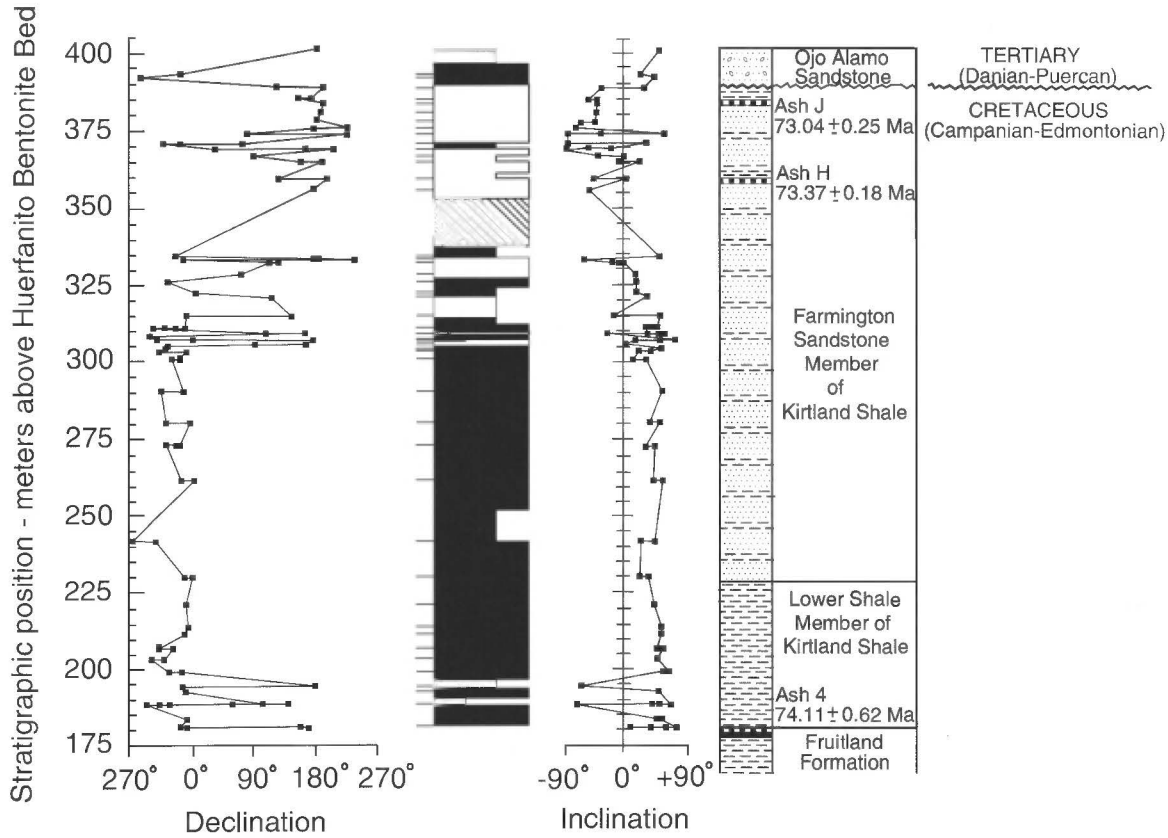

FIGURE 2. Hunter Wash magnetostratigraphic data. Black is normal, white is reversed polarity, and hachures indicate an unsampled interval. The magnetic-polarity column width indicates the degree of certainty of the polarity interpretations; full column width indicates Cretaceous magnetization of the polarities, two-thirds column width indicates probable Cretaceous magnetization, and one-third column width means some indication of Cretaceous polarity but with high uncertainty. Sample positions are shown by tick marks on the left side of the polarity column. The unconformity at the base of the Tertiary Ojo Alamo Sandstone is at 389 m.

sembles the Late Cretaceous direction expected for this site (333.1°, 62.8°) from the cratonic North American paleopole (Gordon, 1995). No mean was calculated for the reversed directions because these generally retained significant overprint magnetization and also constituted a much smaller population of samples. The mean of the normal polarity samples does not resemble Recent or late Tertiary magnetizations for this site. However, the inclinations are significantly shallower than the Cretaceous direction; the inclination shallowness resembles that found in the overlying Nacimiento Formation (Taylor and Butler, 1980), suggesting that perhaps inclination error also may be present in the Fruitland and Kirtland Formations.

A third significant aspect of Hunter Wash paleomagnetism is that the magnetostratigraphic results from this section are nearly identical to those of the section of Butler et al. (1977; Lindsay et al., 1981) in Alamo Wash, 3 km to the east (Fig. 1). In both studies, the polarity reversal boundary is found at essentially the same level: at 325 m in Butler et al. (1977) and at 328 m in this study. Moreover, the observation of several rapid, apparent polarity changes at the normal-to-reversed polarity boundary (Fig. 2) also was observed by Butler et al. (1977, fig. 2). Although these changes appear to suggest field polarity changes, several of their characteristics suggest that probably is not true. Most importantly, the reversed polarity magnetization is never clearly defined. Furthermore, samples indicating reversed polarity generally displayed normal-polarity Cretaceous magnetization directions as removed magnetization between demagnetization steps.

Similar behavior also is exhibited in the basal part of the Hunter Wash section, shown as uncertain reversed polarity in Figure 2. Like the samples exhibiting apparent rapid polarity changes near the polarity boundary, the basal samples of uncertain reversed polarity also display poorly defined reversed polarity which is characterized by intermittent removal of normal polarity magnetization during demagnetization. Both the normal polarity samples underlying the mixed polarity zone and those surrounding the uncertain reversed polarity basal samples have clearly defined normal polarity Cretaceous magnetizations. The poor definition of the reversed polarity magnetization, observation of normal polarity magnetization during the demagnetization of these reversed polarity samples, and the simple univectorial nature of the adjacent normal polarity sample remanences suggest that the reversed polarity in both instances is a secondary magnetization overprinted on an earlier normal polarity magnetization. For these reasons, the apparent alternations of polarity are not regarded as representing primary magnetizations, but remagnetization of discrete packets of normally magnetized strata after the field change to a succeeding reversed polarity interval.

Chimney Rock

At this site, initial directions of magnetization largely clustered around the present magnetic field direction (11.9°, 64.1°), with the exception of samples from the three short segments constituting the upper part of the section; initial directions of samples from those segments clearly represent Cretaceous magnetizations. The initial magnetization intensities of most samples were fairly weak, averaging 4×10^{-4} A/m; the samples that did not mimic the present field direction had somewhat weaker intensities, about 1×10^{-4} A/m. Despite weaker intensities, demagnetization behavior was similar to that at Hunter Wash, and characteristic magnetizations resided in a similar temperature range, 190° to 300–335°C.

The polarity boundary at Chimney Rock (Fig. 3) cannot be determined with as much certainty as at Hunter Wash for several reasons. Fewer samples were collected at Chimney Rock because of the difficulty of sampling the dominantly shale lithology. In addition, a larger number (25%) of the Chimney Rock samples, as compared to Hunter Wash samples (14%), displayed characteristic directions identical to recent magnetizations. Moreover, a large stratigraphic interval of samples between those of single component normal polarity magnetization and those of reversed polarity carries dual polarity magnetizations. Sample magnetization characteristics in this interval are similar to those of apparently mixed polarity observed at Hunter Wash; in both sections, mixed polarity samples occur between the

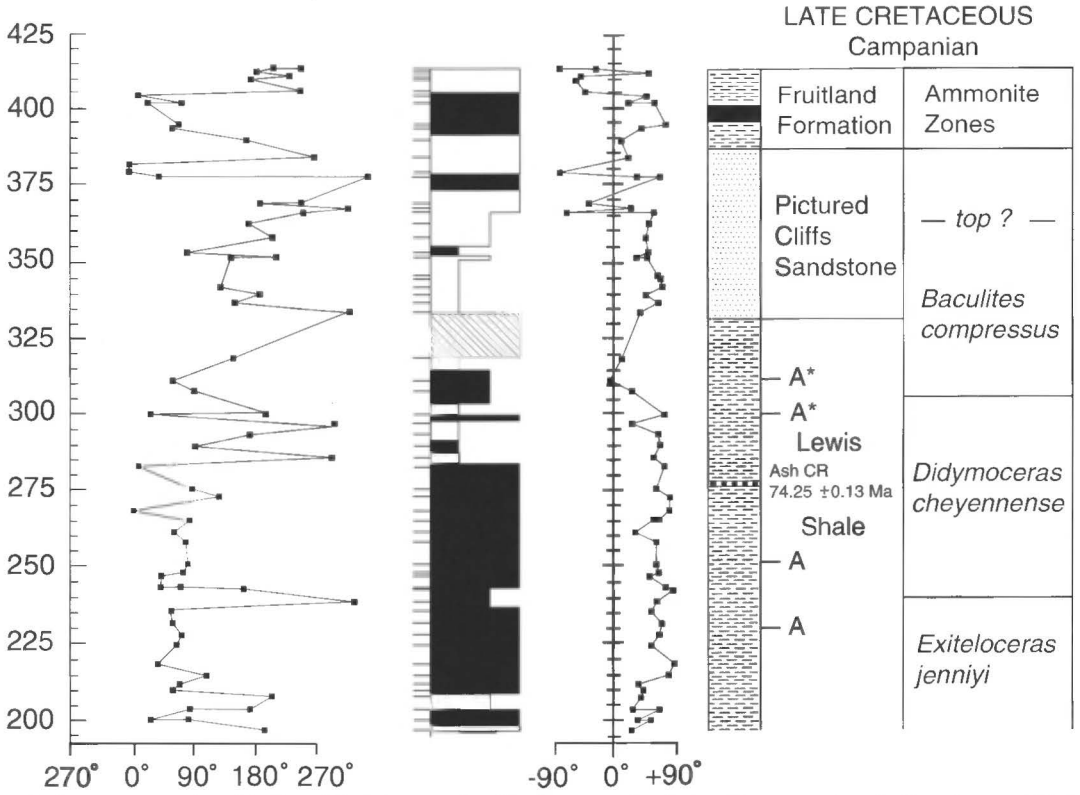

FIGURE 3. Chimney Rock magnetostratigraphic data. Black is normal, white is reversed polarity. The magnetic-polarity column width indicates the degree of certainty of the polarity interpretations; full column width indicates Cretaceous magnetization of the polarities, two-thirds column width indicates probable Cretaceous magnetization, and one-third column width means some indication of Cretaceous polarity but with high uncertainty. Sample positions are shown by tick marks on the left side of the polarity column. Level of volcanic ash bed CR and its $^{40}Ar/^{39}Ar$ age is shown. A's to the right of the lithologic column in the Lewis Shale designate levels of ammonite collections; A's with asterisks indicate ammonite collections from Cobban et al. (1974). Interval colored black in the lithologic column is a Fruitland coal bed.

TABLE 1. Analytical data for $^{40}Ar/^{39}Ar$ age determinations for six San Juan Basin altered volcanic ash beds from the Hunter Wash area in New Mexico and the Chimney Rock area in Colorado.

Ash bed name and J value	Irradiation number	Mineral analysis	Exp. number	40Ar/39Ar	37Ar/39Ar	36Ar/39Ar	K/Ca	%40Ar*	40Ar*/39Ark	Age (Ma)	1 sigma
Ash bed J	JD022	Sanidine	96Z0082	5.84251	0.009032	0.000174	54.2	98.98	5.78315	74.08	0.30
(Fassett K/T)		single Xtl	96Z0085	5.71103	0.007369	0.000006	66.5	99.82	5.70112	73.05	0.26
J=0.006346			96Z0086	5.72075	0.009275	0.000009	52.8	99.81	5.71022	73.16	0.32
			96Z0087	5.72830	0.008386	0.000086	58.4	99.41	5.69492	72.97	0.41
			96Z0088	5.91112	0.013007	0.000050	37.7	99.61	5.88880	75.40	0.26
			96Z0089	5.73928	0.009932	0.000181	49.3	98.93	5.67799	72.75	0.29
			96Z0090	5.73461	0.009117	0.000024	53.7	99.73	5.71939	73.27	0.28
									Unweighted mean and standard deviation w/o errors in J	73.04	0.20
									Weighted mean and weighted standard deviation w/o errors in J	73.05	0.20
									Unweighted mean and error of the mean at the 95% confidence level including the error in J	**73.04**	**0.25**
Ash bed H(1)	JD06	Sanidine	91Z1277	5.98932	0.003994	0.000074	122.7	99.49	5.95875	73.36	0.26
(Hunter Wash 6)		single Xtl	91Z1278	6.08627	0.003978	0.000412	123.2	97.85	5.95573	73.32	0.28
J=0.006965			91Z1280	5.99126	0.005336	0.000101	91.8	99.36	5.95270	73.29	0.26
			91Z1281	5.95985	0.003085	0.000006	158.9	99.82	5.94926	73.24	0.25
			91Z1282	5.97041	0.004894	0.000016	100.1	99.77	5.95695	73.34	0.30
									Unweighted mean and standard deviation w/o errors in J	73.31	0.05
									Weighted mean and weighted standard deviation w/o errors in J	73.31	0.05
									Unweighted mean and error of the mean at the 95% confidence level including the error in J	73.31	0.21
Ash bed H(2)	JD06	Sanidine	91Z1283	5.97047	0.004577	0.000052	107.1	99.60	5.94633	73.54	0.24
(Hunter Wash 10)		single Xtl	91Z1284	5.97268	0.003751	0.000093	130.6	99.39	5.93637	73.42	0.27
J=0.006997			91Z1285	5.95048	0.004290	0.000056	114.2	99.57	5.92504	73.28	0.54
			91Z1286	5.95753	0.004314	0.000014	113.6	99.78	5.94464	73.52	0.34
			91Z1287	5.96512	0.010414	0.000054	47.1	99.72	5.96512	73.77	0.40
									Unweighted mean and standard deviation w/o errors in J	73.51	0.18
									Weighted mean and weighted standard deviation w/o errors in J	73.51	0.14
									Unweighted mean and error of the mean at the 95% confidence level including the error in J	73.51	0.34
									Mean age and uncertainty for two samples sets, H(1) and H(2) (standard error of mean)	73.37	0.08
									Mean age and uncertainty for two samples sets, H(1) and H(2) (95% confidence level)	**73.37**	**0.18**
Ash bed 4	JD010	Sanidine	93Z0350	5.18798	0.021219	0.000031	23.1	99.68	5.1714	74.32	0.27
(Kirtland 86-0-07)		multiple xtls	93Z0351	5.17577	0.033712	0.000062	14.5	99.52	5.15105	74.04	0.29
J=0.008133			93Z0352	5.17808	0.024352	0.000037	20.1	99.65	5.16006	74.16	0.24
			93Z0353	5.18418	0.023203	0.000044	21.1	99.61	5.16388	74.22	0.33
			93Z0354	5.20419	0.035908	0.000212	13.7	98.68	5.13538	73.82	0.37
									Unweighted mean and standard deviation w/o errors in J	74.11	0.19
									Weighted mean and weighted standard deviation w/o errors in J	74.14	0.17
									Unweighted mean and error of the mean at the 95% confidence level including the error in J	**74.11**	**0.62**
Ash bed 2(1)	JD010	Sanidine	93Z0355	5.21431	0.016830	0.000068	29.1	99.47	5.18647	74.36	0.26
(Kirtland 86-0-05)		multiple xtls	93Z0356	5.20874	0.022911	0.000029	21.4	99.70	5.19303	74.46	0.25
J=0.008114			93Z0357	5.20897	0.032658	0.000096	15.0	99.33	5.17419	74.19	0.27
			93Z0358	5.22023	0.020443	0.000010	24.0	99.80	5.20991	74.69	0.31
			93Z0359	5.21996	0.012477	0.000100	39.3	99.28	5.18231	74.31	0.30
									Unweighted mean and standard deviation w/o errors in J	74.4	0.19
									Weighted mean and weighted standard deviation w/o errors in J	74.39	0.18
									Unweighted mean and error of the mean at the 95% confidence level including the error	74.40	0.54
Ash bed 2(2)	JD021	Sanidine	95Z0555	5.89423	0.007657	0.000175	64.0	98.98	5.83445	74.59	0.32
(Kirtland 86-0-05)		single Xtl	95Z0556	5.86859	0.007135	0.000071	68.7	99.50	5.83945	74.65	0.23
J=0.007235			95Z0557	6.09035	0.007425	0.000863	66.0	95.68	5.82725	74.50	0.34
			95Z0558	5.95920	0.007210	0.000349	68.0	98.13	5.84797	74.76	0.33
			95Z0559	5.89310	0.006899	0.000121	71.0	99.25	5.84918	74.77	0.31
			95Z0560	5.86243	0.005295	0.00002	92.5	99.75	5.84805	74.76	0.25
									Unweighted mean and standard deviation w/o errors in J	74.67	0.11
									Weighted mean and weighted standard deviation w/o errors in J	74.68	0.10
									Unweighted mean and error of the mean at the 95% confidence level including the error in J	74.67	0.35
Ash bed 2(3)	JD022	Sanidine	96Z0091	5.88379	0.007845	0.000176	62.5	98.97	5.82352	74.58	0.30
(Kirtland 86-0-05)		single Xtl	96Z0092	5.87229	0.007859	0.000158	62.3	99.06	5.81731	74.50	0.30
J=0.007248			96Z0093	5.87863	0.006452	0.000143	75.9	99.13	5.82790	74.64	0.32
			96Z0094	5.88236	0.007517	0.000135	65.2	99.18	5.83437	74.72	0.28
			96Z0095	5.89134	0.007593	0.000218	64.5	98.76	5.81875	74.52	0.27
			96Z0096	5.83790	0.007549	0.000093	64.9	99.38	5.80227	74.31	0.25
									Unweighted mean and standard deviation w/o errors in J	74.55	0.14
									Weighted mean and weighted standard deviation w/o errors in J	74.53	0.15
									Unweighted mean and error of the mean at the 95% confidence level including the error in J	74.55	0.16
									Mean age and uncertainty for three samples sets, 2(1), 2(2), and 2(3) (standard error of mean)	74.56	0.06
									Mean age and uncertainty for two samples sets, 2(1), 2(2), and 2(3) (95% confidence level)	**74.56**	**0.13**

TABLE 1. (continued)

Ash bed name and J value	Irradiation number	Mineral analysis	Exp. number	40Ar/39Ar	37Ar/39Ar	36Ar/39Ar	K/Ca	%40Ar*	40Ar*/39Ark	Age (Ma)	1 sigma
Ash DEP	JD010	Sanidine	93Z0365	5.31701	0.009886	0.000057	49.6	99.53	5.29182	75.42	0.27
(Lower Fruitland)		multiple xtls	93Z0366	5.31513	0.006601	0.000002	74.2	99.83	5.30607	75.62	0.21
J=0.008068			93Z0367	5.3147	0.022029	0.000002	22.2	99.85	5.30671	75.63	0.23
			93Z0368	5.32145	0.001855	0.000014	264.2	99.75	5.30832	75.65	0.30
			93Z0369	5.30936	0.009924	0.000016	49.4	99.75	5.29637	75.49	0.28
								Unweighted mean and standard deviation w/o errors in J		75.56	0.10
								Weighted mean and weighted standard deviation w/o errors in J		75.57	0.10
								Unweighted mean and error of the mean at the 95% confidence level including the error in J		**75.56**	**0.41**
Ash CR(1)	JD018	Sanidine	94Z0628	6.66639	0.012451	0.000058	39.4	99.62	6.64129	74.47	0.36
(Chimney Rock 9/6/89)		single Xtl	94Z0629	6.64388	0.012715	0.000002	38.5	99.87	6.63523	74.41	0.21
J=0.006346			94Z0630	6.67716	0.011271	0.000132	43.5	99.29	6.63008	74.35	0.25
			94Z0631	6.72427	0.012361	0.000228	39.6	98.88	6.64877	74.55	0.29
			94Z0632	7.73688	0.011889	0.003877	41.2	85.09	6.58302	73.83	0.34
			94Z0633	6.63383	0.011463	0.000002	42.8	99.87	6.62515	74.29	0.21
			94Z0634	6.67627	0.010826	0.000088	45.3	99.49	6.64201	74.48	0.25
								Unweighted mean and standard deviation w/o errors in J		74.34	0.24
								Weighted mean and weighted standard deviation w/o errors in J		74.36	0.19
								Unweighted mean and error of the mean at the 95% confidence level including the error in J		74.34	0.34
Ash CR(2)	JD018	Sanidine	94Z0581	6.65022	0.011035	0.000052	44.4	99.64	6.62666	74.31	0.26
(Chimney Rock 260)		single Xtl	94Z0582	6.66070	0.011591	0.000148	42.3	99.22	6.60876	74.11	0.24
J=0.006346			94Z0583	6.69819	0.011409	0.000249	43.0	98.78	6.61636	74.20	0.27
			94Z0584	6.67044	0.011849	0.000155	41.4	99.19	6.61667	74.20	0.24
			94Z0586	6.66142	0.010789	0.000075	45.4	99.54	6.63092	74.36	0.28
			94Z0587	6.73294	0.012570	0.000374	39.0	98.24	6.61444	74.18	0.26
			94Z0588	6.65070	0.011966	0.000124	41.0	99.33	6.60592	74.08	0.25
			94Z0589	6.67283	0.011058	0.000100	44.3	99.44	6.63525	74.41	0.27
								Unweighted mean and standard deviation w/o errors in J		74.23	0.12
								Weighted mean and weighted standard deviation w/o errors in J		74.22	0.12
								Unweighted mean and error of the mean at the 95% confidence level including the error in J		74.23	0.19
								Mean age and uncertainty for two samples sets, CR(1) and CR(2) (standard error of mean)		74.25	0.06
								Mean age and uncertainty for two samples sets, CR(1) and CR(2) (95% confidence level)		**74.25**	**0.13**

40Ar* in table = radiogenic argon

Ca and K corrections and decay constants

$(^{36}Ar/^{37}Ar)_{Ca}=2.69 \pm 0.24 \times 10^{-4}$

$(^{39}Ar/^{37}Ar)_{Ca}=6.79 \pm 0.051 \times 10^{-4}$

$(^{40}Ar/^{39}Ar)_{K}=9.1 \pm 5.4 \times 10^{-3}$

$\lambda_{\varepsilon} + \lambda_{\varepsilon'} = 0.581 \times 10^{-10}\ yr^{-1}$

$\lambda_{\beta} = 4.962 \times 10^{-10}\ yr^{-1}$

$^{40}K/K = 1.167 \times 10^{-4}$ atom/atom

NOTE: Underlined numbers shown for ash J in the "Age (Ma)" and "1 sigma" columns were excluded from the weighted-mean age determination for this ash bed

clearly normal and clearly reversed polarity samples, suggesting a continuation of magnetization in the succeeding polarity interval after deposition. If this is the correct explanation, it suggests that post-depositional magnetization may have continued longer at Chimney Rock compared with Hunter Wash. Regardless of the origin, the large stratigraphic interval of mixed polarity magnetization creates significant uncertainty as to the exact location of the polarity boundary at Chimney Rock, and can only be determined to reside somewhere within the interval of 285 m to 366 m (Fig. 3).

Isotopic dating

Samples of altered volcanic ash layers were collected at several levels at the Hunter Wash and Chimney Rock sites. Generally, ash layers were purer at the bottom and somewhat contaminated with clastic and organic material at the top; the ages reported here were obtained only from the purer basal part of each ash layer. All of the ages were determined by John Obradovich, U.S. Geological Survey, Denver, Colorado. Sanidine crystals were separated from the ashes and dated using the $^{40}Ar/^{39}Ar$ laser fusion method (methodology described in Obradovich, 1993). Most analyses were of single crystals but some were of multiple crystals (Table 1).

Five datable ash beds were found in the Hunter Wash area (Figs. 1, 2). The lowest ash (ash DEP), is 18 cm thick and is in the upper part of the stratigraphically lowest outcropping Fruitland Formation coal bed in the San Juan Basin at 36°11.35' N lat., 108°10.28' W long., near Dog Eye Pond (Tanner Lake Quadrangle, New Mexico). Ash 2 also is 18 cm thick and is at the top of a middle Fruitland coal bed in Hunter Wash at 36°17.74' N lat., 108°13.46' W long., about 3.9 km downstream from the starting point of our Hunter Wash paleomagnetic traverse. Ash 4 is 34 cm thick and is at the top of a coal bed at the top of the Fruitland Formation (this locality is the starting point for the Hunter Wash paleomagnetic traverse). Ash H is 20 cm thick and was collected from the base of a chocolate-brown mudstone in the upper part of the Farmington Sandstone Member of the Kirtland Shale at 36°21.63' N lat., 108°36' W long. Ash J is 21 cm thick and is overlain by a chocolate-brown mudstone very near the top of the Farmington Member of the Kirtland Shale at 36°21.86' N lat., 108°07.88' W long. Collection sites for the latter four ash layers are in the Alamo Mesa West Quadrangle, New Mexico. Sample levels and $^{40}Ar/^{39}Ar$ ages for the five Hunter Wash ash beds are (Figs. 2, 4; Tables 1, 2): ash DEP, 29 m, 75.56 ± 0.41 Ma; ash 2, 136 m, 74.56 ± 0.13 Ma; ash 4, 181 m, 74.11 ± 0.62 Ma;

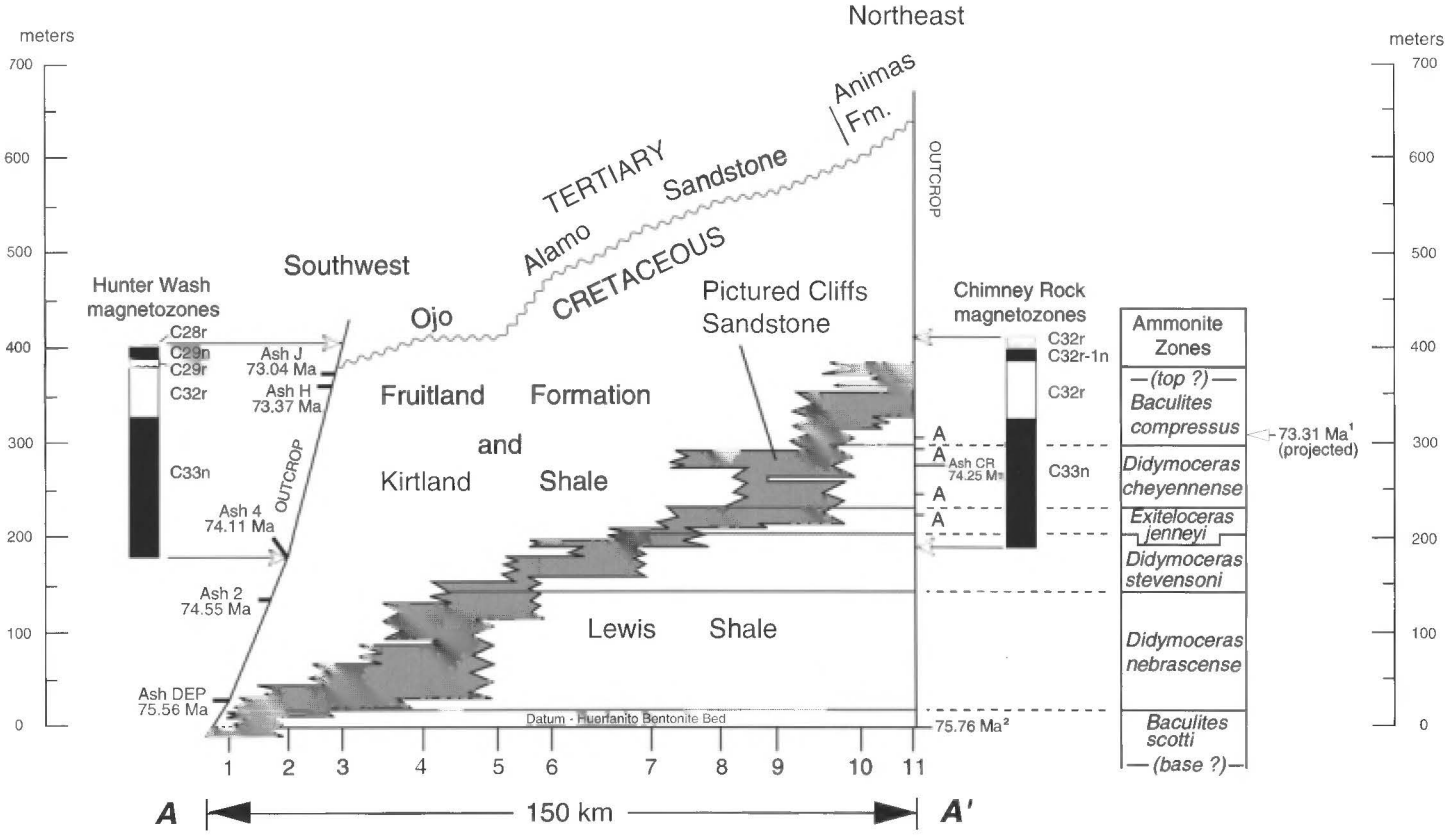

[1] *Baculites compressus* age is from a bentonite bed in the Bearpaw Shale, Big Horn County, Montana (Obradovich, 1993 and written communication, Obradovich, 1996).

[2] Age of Huerfanito Bentonite Bed from a sample from east side, San Juan Basin, about 19 km northeast of Cuba, New Mexico (Fig. 1 and Fassett and others, 1977, this volume) Huerfanito age from Obradovich (1993) and written communication, Obradovich (1996).

FIGURE 4. Stratigraphic cross section A–A' (trace on Fig. 1). Drill holes used for control for construction of this cross section are listed in Table 2. Levels and ages of altered volcanic ash beds DEP, 2, 4, H, and J at Hunter Wash and CR at Chimney Rock are shown. Letters A at the Chimney Rock section show levels of ammonite collection sites. Ammonite zone boundaries for *Baculites compressus/ Didymoceras cheyennense* and *D. cheyennense/Exiteloceras jenneyi* are based on collections at Chimney Rock. Stratigraphically lower ammonite zone boundaries shown are from Fassett (1987) based on collections described in Cobban (1973) and Cobban et al. (1974). Magnetostratigraphic interpretations are simplifications of Figures 3 and 4; black is normal polarity, white is reversed. At Chimney Rock the C33n-C32r polarity reversal is shown at the approximate midpoint of the 285 to 366-m zone containing the polarity reversal.

ash H, 359 m, 73.37 ± 0.18 Ma, and ash J, 384 m, 73.04 ± 0.25 Ma. Ash J is only 4.9 m below the base of the Ojo Alamo Sandstone (as described in Fassett, 1987).

An ash bed 2.5 cm thick, sampled from the uppermost part of the Lewis Shale at the Chimney Rock location (Figs. 3, 4) at 277 m yielded a $^{40}Ar/^{39}Ar$ sanidine-crystal age of 74.25 ± 0.13 Ma (Table 1).

Paleontology

Hunter Wash is in the western part of a classic vertebrate fossil area centered on Alamo Wash about 3 km east of Hunter Wash (Fig. 1). We found dinosaur bone fragments (not collected or identified) at many levels in the Kirtland Shale and the lower part of the Ojo Alamo Sandstone in the course of our Hunter Wash traverse. Collections of vertebrate remains from this area were described by Clemens (1973), Lucas et al. (1987), and Hunt and Lucas (1992). Palynomorphs from this area have been identified by Anderson (1960); further collections from the area were identified by R. S. Tschudy of the U.S.G.S., which are listed and discussed in Fassett et al. (1987).

Although vertebrate fossils are abundant in the vicinity of our Hunter Wash section, their value in fixing the biostratigraphic age of the rocks containing the polarity reversal (Kirtland Shale) is limited. Faunal data from this area have been difficult to interpret because of the endemic nature of taxa and uncertainties in differentiating between geographic and age differences in faunal assemblages (Lucas et al., 1987). However, Hunt and Lucas (1992, p. 234) concluded that "...the lower Kirtland is Edmontonian (early Maestrichtian) in age"; moreover, their figure 11 shows *all* of the upper Kirtland Shale (of this report) to be Edmontonian. Palynological data are not definitive regarding the exact age of the strata containing the reversal but essentially are in agreement with vertebrate fossil evidence.

At the Chimney Rock section, marine macrofossils from the Lewis Shale were collected and identified for this study by William A. Cobban, U.S.G.S., Denver, Colorado; this work augmented earlier studies by Cobban (1973) and Cobban et al. (1974). Ammonite collection data from the Lewis Shale throughout the San Juan Basin are synthesized in Fassett (1987). Samples of the Lewis Shale at the Chimney Rock locality were analyzed for marine microfossils but no age-diagnostic fossils were found. The few foraminifers and ostracodes present in these samples were indicative of a nearshore, normal-salinity, shallow-water environment (less than 90 m water depth, written commun., 1994, M. A. Carey and E. Brouwers).

Fossil collections from the Lewis Shale at Chimney Rock include *Exiteloceras jenneyi* (Whitfield) at 230 m and *Baculites undatus* Stephenson at 251 m; *B. undatus* has not been found to occur lower than the *D. cheyennense* zone. An assemblage consisting of *Inoceramus* aff. *I. convexus* Hall and Meek, *Ostrea inornata* Meek and Hayden, *Placenticeras* sp., *Baculites* aff. *B. rugosus* Cobban, *Didymoceras* cf. *D. cheyennense* (Meek and Hayden), and *Oxybeloceras*? sp. occurs at 300 m; this assemblage is probably the zone of *D. cheyennense* (Cobban et al., 1974). An assemblage consisting of *Inoceramus* aff. *I. barabini* Morton, *Ostrea* sp., *Syncyclonema hallii* (Gabb) (a small pecten), *Eutrephoceras* sp. (a nautiloid), *Placenticeras meeki* Boehm, *Baculites compressus* Say?, and *Hoploscaphites* sp. occurs at 312 m, which probably represents the zone of *B. compressus* (Cobban et

TABLE 2. List of drill holes used for control for cross section A–A' (Figs. 1, 4).

Number	Company	Well name	Section	Township(N)	Range(W)
1	U.S. Geological Survey	Tanner Lake 27-1*	27	23	13
2	Tesoro Petroleum Corp.	Nariz 1 Federal	30	24	12
3	Shell Oil Co.	Government 41-21	21	25	12
4	El Paso Naural Gas Co.	Delhi-Taylor Pool Unit 1-D	3	26	11
5	Sunset International Petroleum Corp.	Sipco Kutz Federal 2-F	4	27	10
6	El Paso Naural Gas Co.	Reid 1	8	28	9
7	Delhi Oil Corp.	C.J. Moore 1	8	30	8
8	Northwest Pipeline Corp.	San Juan 32-7 Unit 79	7	31	7
9	El Paso Naural Gas Co.	Allison 24	7	32	6
10	Sun Oil Co.	Wright 1	16	33	5
11	Big Horn Powder River Corp.	Schomberg 1	14	34	5

*Geophysical log and core description for the USGS Tanner Lake 27-1 drill hole in Jentgen and Fassett (1977)

al., 1974). On the basis of these data, the ammonite zone boundaries at Chimney Rock (Fig. 3) are established as *E. jenneyi/D. cheyennense* at 240 m and *D. cheyennense/B. compressus* at 306 m. The polarity reversal at Chimney Rock thus most likely falls in the lower part of the *B. compressus* zone, although it may be in the uppermost part of the *D. cheyennense* zone.

DISCUSSION

Stratigraphy

The basin-wide relations of the rocks containing the polarity reversals are shown on a northeast-trending stratigraphic cross section from Hunter Wash to Chimney Rock (Fig. 4). Subsurface stratigraphic relations are based on 11 geophysical logs from drill holes evenly spaced across the basin (Figs. 1, 4). This 147-km-long cross section is generally at right angles to the depositional strike (Pictured Cliffs Sandstone shoreline trends, Fassett, 1987). Relative to the Huerfanito Bed datum, the top of the Pictured Cliffs Sandstone rises 395 m stratigraphically across the basin, from a projected level of 5 m below the Huerfanito Bed just south of Dog Eye Pond to 390 m above the Huerfanito Bed at Chimney Rock (Fig. 4).

At Hunter Wash, ash J, 73.04 ± 0.25 Ma age, is 4.9 m below the base of the Ojo Alamo Sandstone (Figs. 1, 2). The upper part of the Ojo Alamo Sandstone interfingers with the lower part of the Nacimiento Formation, which contains a Puercan (early Paleocene) mammal fauna (Hunt and Lucas, 1992); thus, based on this data the Ojo Alamo is early Paleocene in age. Palynologic sample data from the Ojo Alamo, summarized by Fassett et al. (1987), also indicate an early Paleocene age for the Ojo Alamo Sandstone. A recent estimate for the age of the Cretaceous-Tertiary boundary is 65.4 ± 0.1 Ma (Obradovich, 1993), therefore, an 8 Ma hiatus is present within the thin interval between ash J and the base of the Ojo Alamo Sandstone. We conclude that this hiatus probably occurs at the base of the Ojo Alamo Sandstone.

Age and identity of polarity reversal

The change from normal to reversed polarity in the Hunter Wash section occurs at about 328 m, which is in the upper part of the Farmington Sandstone Member of the Kirtland Shale (Fig. 2). The polarity reversal is bracketed by ash beds 4 and H; these ashes are separated by 178 m stratigraphically and 0.74 Ma in time. The reversal is 31 m below ash H and 147 m above ash 4. At a linear rate of sediment accumulation, the interpolated age of the polarity reversal at Hunter Wash is 73.50 ± 0.18 Ma (interpolated uncertainty determined by the technique of Renne et al., 1993). The reversal age using five other possible combinations of bracketing ages from the five Hunter Wash ash beds (2 above and 3 below the reversal) are: ashes H/2, 73.54 ± 0.16 Ma; H/DEP, 73.58 ± 0.17 Ma; J/4, 73.34 ± 0.25 Ma; J/2, 73.38 ± 0.20 Ma; and ash J/DEP, 73.44 ± 0.22 Ma. The average age from all estimations is 73.46 ± 0.18 Ma, identical to the age estimated from the two bracketing ash layers.

At Chimney Rock, the polarity of magnetization changes from normal to reversed within the Lewis Shale between 285 and 366 m (Fig. 3). Ash CR, of 74.25 ± 0.13 Ma age, is at 277 m, just below the stratigraphic interval of the polarity change. Although the exact level of the reversal cannot be pinpointed at Chimney Rock, the age of the midpoint of the probable reversal interval is 73.50 Ma (extrapolated from the CR-ash age at a rate of deposition of 65 m/my).

Work by Obradovich (1993) provides revised ages for many of the Western Interior ammonite zones. That work, and more recent refinements (Obradovich, written commun., 1995), indicates that the age of the *B. compressus* zone in the Western Interior is 73.31 ± 0.35 Ma. The polarity reversal at Chimney Rock appears to be in the lower part of the *B. compressus* zone (Fig. 4); thus, our extrapolated age for the reversal at Chimney Rock of 73.50 Ma is in close agreement with Obradovich's age for the *B. compressus* ammonite zone of 73.31 Ma.

The normal polarity interval (Fig. 2) preceding the reversal at Hunter Wash represents about 0.6 Ma (147 m deposited at a rate of 249 m/Ma). Only two normal polarity intervals of this duration—C32n and C33n—are present in the upper Campanian to lower Maestrichtian (Cande and Kent, 1992, 1995). Our 73.50 Ma age for the San Juan Basin reversal is essentially the same as the recently-revised age of 73.62 Ma for the reversal bounding chrons C33n-C32r of Cande and Kent (1995). We thus identify the polarity reversal at Hunter Wash and Chimney Rock as the C33n-C32r reversal. Moreover, this result more precisely dates the C33n-C32r reversal as 73.50 (± 0.18) Ma.

Further confirmation that the Hunter Wash-Chimney Rock polarity reversal is the C33n-C32r reversal comes from the observation of a thin, normal-polarity interval in the Fruitland Formation higher in the Chimney Rock section (Figs. 3, 4). The samples from this normal-polarity interval clearly have Cretaceous normal-polarity directions, and the level of this normal-polarity interval above the C33n-C32r reversal is in good agreement with the relative relationship of the C32r–1n normal interval to the C33n-C32r reversal in the Cande and Kent (1995) time scale.

Age of Huerfanito Bentonite Bed

The Huerfanito Bentonite Bed is projected to lie 29 m below the DEP (Dog Eye Pond) ash bed (Figs. 1, 4) in the southwest part of the San Juan Basin. The age of ash DEP is 75.56 ± 0.41 Ma. At a rate of deposition for the interval between the DEP ash and ash 2 of 107 m/Ma, the extrapolated age of the Huerfanito is 75.83 Ma. An ash collected on the east side of the San Juan Basin by C. M. Molenaar (see Fassett et al., this volume) from the Lewis Shale in the *Baculites scotti* ammonite zone yielded an age of 75.89 ± 0.72 Ma (Obradovich, 1993); this ash was recently redated at 75.76 ± 0.34 Ma (Obradovich, written commun., 1995). C. M. Molenaar (oral commun., 1994) inferred that this ash was the Huerfanito Bentonite Bed; the virtual agreement of the extrapolated age of the Huerfanito at Dog Eye Pond and the actual age of the Molenaar ash bed on the east side of the basin tends to confirm Molenaar's conclusion that the outcropping ash bed is the Huerfanito. This result is significant because the Huerfanito has never been positively identified on the outcrop in the San Juan Basin and hence never precisely dated. This finding also confirms that the Huerfanito Bed occurs in the *B. scotti* zone at Dog Eye Pond (as projected on Fig. 4).

Comparison with previous work

As mentioned above, a paleomagnetic traverse was conducted in Alamo Wash, a drainage parallel to and 3 km east of Hunter Wash (Fig. 1), by Butler et al. (1977); subsequent paleomagnetic collections were made at other sites in the San Juan Basin (see Lindsay et al., 1978; Taylor and Butler, 1980; Lindsay et al., 1981, 1982; Butler and Lindsay, 1985). The change from normal to reversed polarity at Alamo Wash was identified by these authors as the C30n–C29r reversal. The reversal we observe in Hunter Wash is clearly the same reversal detected by Butler et al. (1977) in Alamo Wash.

Identification of the Alamo Wash reversal as C30n-C29r in the above-cited papers was based in part on a comparison of the San Juan Basin magnetostratigraphic pattern to the sea-floor spreading magnetic polarity pattern and the magnetostratigraphic sequence at Gubbio, Italy. Biochronologic and fission-track-dating data from the Alamo Wash area were cited in support of the C30n-C29r polarity-reversal identification there. As a result of the identification of this reversal in the upper Kirtland Shale as C30n-C29r, these authors concluded that deposition across the Cretaceous-Tertiary boundary in the southern San Juan Basin must have been continuous, inconsistent with the findings of many earlier workers who had concluded that a significant hiatus was present at the K-T boundary in the San Juan Basin.

Many critical responses followed publication of this interpretation of continuous deposition, e.g., Rigby and Lucas (1977), Alvarez and Vann (1979), Fassett (1979, 1982), Lucas and Rigby (1979), Lucas and Schoch (1982) and Fassett and Obradovich (1986). Ultimately, a collection of papers on the K-T boundary in the San Juan and Raton Basins was published (Fassett and Rigby, 1987) that significantly challenged the concept of continuous deposition across the K-T boundary in the San Juan Basin, and hence the identification of the reversal at Hunter Wash as C30n-C29r. Our present study conclusively demonstrates that the polarity reversal in the upper Kirtland Shale in Hunter Wash and Alamo Wash is C33n-C32r and documents the presence of an 8 Ma hiatus at the base of the Tertiary Ojo Alamo Sandstone at Hunter Wash.

Hunt and Lucas (1992) presented a lengthy and forceful discussion of the age of the Fruitland Formation, Kirtland Shale, and associated rocks based primarily on vertebrate assemblages collected over the years from these formations. One of their conclusions was that "Given the vertebrate evidence, there is only space for 3 million years to be missing at the base of the Ojo Alamo . . ." (Hunt and Lucas, 1992, p. 235). They further stated that the hiatus is probably much less than 3 million years and concluded that " . . . there is no major angular unconformity at the base of the Ojo Alamo Sandstone in the San Juan Basin." The data presented in this report demonstrate that there is an 8 Ma hiatus within the 4.5-m rock interval immediately beneath the base of the Ojo Alamo Sandstone at Hunter Wash; this data, however, cannot be used to assess the angularity of this substantial unconformity.

Hicks (1993) reported that the C33n-C32r polarity reversal was present in the *Exiteloceras jenneyi* ammonite zone of the Pierre Shale at Red Bird, Wyoming, at a section studied in detail by Gill and Cobban (1966). Hicks showed a 420-m section of normal-polarity strata at this locality overlain by 5 m of somewhat less well defined reversed-polarity strata (Hicks 1993; oral commun., 1994). The short interval of reversed polarity is truncated by a 2.5 Ma hiatus (Obradovich, 1993, fig. 2), representing possibly the upper part of the *E. jenneyi* zone, all of the *Didymoceras cheyennense*, *Baculites compressus*, and *B. cuneatus* zones, and possibly the lower part of the *B. reesidei* zone (Gill and Cobban, 1966).

In the San Juan Basin, the *E. jenneyi* zone and most, if not all, of the overlying *D. cheyennense* zone occur within a normal polarity interval. Recently, 11 samples were collected from the Pierre Shale at Red Bird, Wyoming, at 0.01 m above to 13.5 m below the unconformity. Many of these samples exhibited unambiguous, normal-polarity, Cretaceous magnetization; two samples showed ambiguous (not clearly Cretaceous) reversed polarity magnetization, and the remainder, a messy multi-component magnetization (Steiner, Shoemaker and Cobban, unpublished data, 1996). Of three samples taken in the bed directly overlying the hiatus, two had normal, and one, reversed polarity. The origin of the reversed-polarity magnetization observed by Hicks just below the unconformity is unclear. The new data for this interval suggest that Hicks' reversed-polarity samples might represent secondary magnetization related to the unconformity or possibly a remagnetization during the time of the succeeding reversed-polarity interval, similar to that observed in the San Juan Basin sections of the present study. We suggest that the reversed-polarity strata of Hicks (1993) just beneath the unconformity at Red Bird may not represent the base of chron C32r.

CONCLUSIONS

This study establishes the age of the C33n-C32r polarity reversal as 73.50 ± 0.18 Ma. This result provides a new Upper Cretaceous tie point for more precise refinement of geologic time scales. The determination that the C33n-C32r reversal apparently occurs in the lower part of the *Baculites compressus* zone now allows direct correlation of the endemic Western Interior ammonites to the open-ocean faunal zones in Europe and elsewhere in the world. In addition, the identification of the C33n-C32r reversal in marine and continental rocks in the San Juan Basin offers the first direct link between the tightly age-controlled ammonite zones of the marine realm of the Western Interior and the faunal and floral zones in time-equivalent continental rocks. Furthermore, the faunal and floral assemblages present in the Fruitland and Kirtland can now be related to other such faunal assemblages throughout the Western Interior wherever the C33n-C32r reversal can be found or precise radiometric ages determined. An 8 Ma hiatus has been documented in the San Juan Basin within the uppermost 5 m of the Kirtland Shale at Hunter Wash; this hiatus is most likely located at the base of the early Paleocene Ojo Alamo Sandstone.

ACKNOWLEDGMENTS

This study was funded by a U.S. Geological Survey Gilbert Fellowship awarded to Fassett in 1988. Our sincere thanks go to USGS geologists John Obradovich for providing the ages for the six dated ash beds discussed in the report, William A. Cobban for identification of ammonites from the Chimney Rock area, and to Mary Alice Carey and Elisabeth M. Brouwers for their work on the Lewis Shale microfossils from the Chimney Rock section. Special thanks go to Glen Rabey of the U.S. Forest Service, Pagosa Springs, Colorado, for providing access to the Chimney Rock archeological site.

REFERENCES

Alvarez, W. and Vann, D. W., 1979, Comment on "Biostratigraphy and magnetostratigraphy of Paleocene terrestrial deposits, San Juan Basin, New Mexico": Geology, v. 7, p. 66–67.

Butler, R. F. and Lindsay, E. H., 1985, Mineralogy of magnetic minerals and revised magnetic polarity stratigraphy of continental sediments, San Juan Basin, New Mexico: Journal of Geology, p. 535–554.

Butler, R. F., Lindsay, E. H., Jacobs, L. L. and Johnson, N. M., 1977, Magnetostratigraphy of the Cretaceous-Tertiary boundary in the San Juan Basin, New Mexico: Nature, v. 267, p. 318–323.

Cande, S. C. and Kent, D. V., 1992, A new geomagnetic polarity time scale for the Late Cretaceous and Cenozoic: Journal of Geophysical Research, v. 97, no. B10, p. 13,917–13,951.

Cande, S. C. and Kent, D. V., 1995, Revised calibration of the geomagnetic polarity timescale for the Late Cretaceous and Cenozoic, Journal of Geophysical Research, v. 100, no. B4, p. 6093–6095.

Clemens, W. A., 1973, The roles of fossil vertebrates in interpretation of Late Cretaceous stratigraphy of the San Juan Basin, New Mexico; *in* Fassett, J. E., ed., Cretaceous and Tertiary rocks of the southern Colorado Plateau: Four Corners Geological Society Memoir, p. 154–167.

Cobban, W. A., 1973, Significant ammonite finds in uppermost Mancos Shale and overlying formations between Barker Dome, New Mexico and Grand Junction, Colorado; *in* Fassett, J. E., ed., Cretaceous and Tertiary rocks of the southern Colorado Plateau: Four Corners Geological Society Memoir, p. 148–153.

Cobban, W. A., Landis, E. R. and Dane, C. H., 1974, Age relations of upper part of Lewis Shale on east side of San Juan Basin, New Mexico: New Mexico Geological Society, Guidebook 28, p. 279–282.

Fassett, J. E., 1979, Comment on "Biostratigraphy and magnetostratigraphy of Paleocene terrestrial deposits, San Juan Basin, New Mexico": Geology, v. 7, p. 69–70.

Fassett, J. E., 1982, Dinosaurs in the San Juan Basin, New Mexico, may have survived the event that resulted in creation of an iridium-enriched zone near the Cretaceous/Tertiary boundary: Geological Society of America, Special Paper 190, p. 435–447.

Fassett, J. E., 1987, The ages of the continental, Upper Cretaceous, Fruitland Formation and Kirtland Shale based on a projection of ammonite zones from the Lewis Shale, San Juan Basin, New Mexico and Colorado: Geological Society of America, Special Paper 209, p. 5–16.

Fassett, J. E., Cobban, W. A. and Obradovich, J. D., 1997, Biostratigraphic and isotopic age of the Huerfanito Bentonite Bed of the Upper Cretaceous Lewis Shale at an outcrop near Regina, New Mexico: New Mexico Geological Society, Guidebook 48.

Fassett, J. E. and Hinds, J. S., 1971, Geology and fuel resources of the Fruitland Formation and Kirtland Shale of the San Juan Basin, New Mexico and Colorado: U.S. Geological Survey, Professional Paper 676, 76 p.

Fassett, J. E. and Obradovich, J. D., 1986, A high precision $^{40}Ar/^{39}Ar$ age-spectrum plateau of 74 Ma from the uppermost, Upper Cretaceous Fruitland Formation-Kirtland Shale, identifies paleomagnetic Chron 33-normal in the San Juan Basin, New Mexico: Geological Society of America, Abstracts with Programs, v. 17, p. 599.

Fassett, J. E., Lucas, S. G. and O'Neill, F. M., 1987, Dinosaurs, pollen and spores, and the age of the Ojo Alamo Sandstone, San Juan Basin, New Mexico: Geological Society of America, Special Paper 209, p. 17–34.

Fassett, J. E. and Rigby, J. K., Jr., eds., 1987, The Cretaceous-Tertiary boundary in the San Juan and Raton Basins, New Mexico and Colorado: Geological Society of America, Special Paper 209, 200 p.

Gill, J. R. and Cobban, W. A., 1966, The Red Bird section of the Upper Cretaceous Pierre Shale in Wyoming: U.S. Geological Survey, Professional Paper 393-A, 73 p.

Gordon, R. G. and Van der Voo, R., 1995, Mean paleomagnetic poles for the major continents and the Pacific plate; *in* Ahrens, T. J., ed., Global Earth physics—a handbook of physical constants: American Geophysical Union Shelf Reference, v. 1, p. 225–239.

Hicks, J. F., 1993, Chronostratigraphic analysis of the foreland basin sediments of the latest Cretaceous, Wyoming, U.S.A. [Ph.D. thesis]: New Haven, Yale University, 250 p.

Hunt, A. P. and Lucas, S. G., 1992, Stratigraphy, paleontology, and age of the Fruitland and Kirtland formations (Upper Cretaceous), San Juan Basin, New Mexico: New Mexico Geological Society, Guidebook 43, p. 217–239.

Jentgen, R. W. and Fassett, J. E., 1977, Sundance-Bisti-Star Lake 1976 Drilling in McKinley and San Juan Counties, Northwestern New Mexico: U.S. Geological Survey, Open File Report 77-369, 80 p.

Lindsay, E. H., Jacobs, L. L. and Butler, R. F., 1978, Biostratigraphy and magnetostratigraphy of Paleocene terrestrial deposits, San Juan Basin, New Mexico: Geology, v. 6, p. 425–429.

Lindsay, E. H., Butler, R. F. and Johnson, N. M., 1981, Magnetic polarity zonation and biostratigraphy of Late Cretaceous and Paleocene continental deposits, San Juan Basin, New Mexico: American Journal of Science, v. 281, p. 390–435.

Lindsay, E. H., Butler, R. F. and Johnson, N. M., 1982, Testing of magnetostratigraphy in Late Cretaceous and early Tertiary deposits, San Juan Basin, New Mexico: Geological Society of America, Special Paper 190, p. 435–447.

Lucas, S. G., Mateer, N. J., Hunt, A. P. and O'Neill, F. M., 1987, Dinosaurs, the age of the Fruitland and Kirtland Formations, and the Cretaceous-Tertiary boundary in the San Juan Basin, New Mexico: Geological Society of America, Special Paper 209, p. 35–50.

Lucas, S. G. and Rigby, J. K., Jr., 1979, Comment on "Biostratigraphy and magnetostratigraphy of Paleocene terrestrial deposits, San Juan Basin, New Mexico": Geology, v. 7, p. 323–325.

Lucas, S. G. and Schoch, R. M., 1982, Discussion of magnetic polarity zonation and biostratigraphy of Late Cretaceous and Paleocene continental deposits, San Juan Basin, New Mexico: American Journal of Science, v. 282, p. 920–927.

Obradovich, J. D., 1993, A Cretaceous time scale; *in* Caldwell, W. G. E. and Kauffman, E. G., eds., Evolution of the Western Interior Basin: Geological Association of Canada, Special Paper 39, p. 379–396.

Renne, P., Walter, R., Verosub. K, Sweitzer, M. and Aronson, J., 1993, New data from Hadar (Ethiopia) support orbitally tuned time scale to 3.3 Ma: Geophysical Research Letters, American Geophysical Union, v. 20, p. 1067–1070.

Taylor, L. H. and Butler, R. F., 1980, Magnetic-polarity stratigraphy of Torrejonian sediments, Nacimiento Formation, San Juan Basin, New Mexico: American Journal of Science, v. 280, p. 97–115.

Tschudy, R. H., 1973, The Gasbuggy core—a palynological appraisal; *in* Fassett, J. E., ed., Cretaceous and Tertiary rocks of the southern Colorado Plateau: Four Corners Geological Society Memoir, p. 131–143.